

Pion double charge exchange on ${}^4\text{He}$

M. Alqadi and W. R. Gibbs

Department of Physics, New Mexico State University, Las Cruces, NM, 88003

November 4, 2018

Abstract

The doubly differential cross sections for the ${}^4\text{He}(\pi^+, \pi^-)4p$ reaction were calculated using both a two-nucleon sequential single charge exchange model and an intranuclear cascade code. Final state interactions between the two final protons which were the initial neutrons were included in both methods. At incident pion energies of 240 and 270 MeV the low-energy peak observed experimentally in the energy spectrum of the final pions can be understood only if the contribution of pion production is included. The calculated cross sections are compared with data.

1 Introduction

The pion double-charge exchange (DCX) reaction is one of the rare forms of nuclear reactions which involve a minimum of two nucleons and provides a tool to study two nucleon correlations within a target nucleus. A number of studies have been made of exclusive DCX and interesting results have been obtained in regard to correlations[1] and the propagation of pions through the nucleus in its ground state[2, 3]

In this paper we study inclusive DCX on a well understood nucleus where the principal physics interest lies in understanding and describing the mechanism.

It is essential to be able to describe nuclear reactions on the hadronic level in order to interpret possible deviations from the expected behavior as “new physics” phenomena. Several techniques have been used to describe inclusive DCX. Becker and Schmit [4] used the sequential single charge mechanism in their calculations and their results showed general agreement with the energy dependence of the total cross section but predicted cross sections larger than the experiment data.

Germond and Wilkin[5] suggested a different mechanism for DCX reaction, the interaction of the incident pion with the exchange current meson or pions in the cloud surrounding each nucleon. Their calculations did not include the Pauli effect or Fermi motion of the nucleons. The production mechanism introduced by Jeanneret [6] gave good agreement with DCX cross section at energies above the P_{33} region and may be the main mechanism there.

Gibbs *et al.*[7], reported another attempt to calculate the total and doubly differential cross section for the DCX reaction by using the sequential single charge exchange mechanism. They included a treatment of anti-symmetric wave functions. Both Pauli blocking and a crude form of final state interaction (FSI) were included in their work but interactions with the “spectator” protons were ignored as in the previous cases.

In conjunction with dibaryon searches, Gräter *et al.*[8] calculated the total cross section for ^4He . In their model FSI was taken into account by using a Watson-Migdal Model in an eikonal approximation.

Following the early total DCX cross section data, extensive experimental studies performed at Clinton P. Anderson Meson Physics facility reported high precision results for doubly differential cross sections. The experiments covered a wide range of elements ($A=4, 208$) over a range of incident energies (120 - 270) MeV. These studies showed a two peak structure in the energy spectra at forward angles at the higher energies in the low atomic number elements such as ^4He and ^3He [9, 10], while that structure disappears in the heavier elements ^{16}O , ^{40}Ca [11, 12] .

A number of calculations attempting to explain this two-peaked structure have followed a suggestion by M. Thies. He and Van Loon [13] did calculations based on the fact that the angular distribution of the pion nucleon cross section is dominated by the p-wave and hence has a forward-backward peaked angular distribution in the πN center of mass. In this case, pions coming from the DCX reaction in the forward direction would have made two small angle or two large angle scatterings. Two small angle scatterings would generate only a small energy loss while two large angle scatterings would bring about a large energy loss due to the recoil of the nucleons. This effect surely exists but there have been difficulties with obtaining a quantitative representation of the data using only this model.

Another early attempt to explain the double peak structure in ^4He was by Wood[11] relying

on the mechanism proposed by Thies. Kinney [9] modified the Thies model by including several effects of the nuclear medium. His results gave reasonable quantitative agreement with the shape of the spectrum for ${}^4\text{He}$ for some angles, but did not follow the cross section as a function of angle. Recent calculations carried out by Kulkarni[14], based on a relativized version of the code of Ref.[7], found qualitative agreement with Kinney’s data.

Part of the difficulty with the forward-backward argument is that the scatterings take place over a 3 dimensional sphere, which means that there is factor of $\sin\theta$ arising from the solid angle of the first charge exchange which mitigates the forward-backward angular distribution. Also, at 240 and 270 MeV, where the effect is the strongest, not only does the pion-nucleon angular distribution become more forward peaked in the center of mass as energy increases but it will also be thrown forward in the laboratory so that the backward (corresponding to low energy) peak is much diminished. We will return to this point in the discussion.

2 Two-nucleon Model

We first consider a model in which the two “spectator” protons do not play an active role in the scattering but do influence the result through the energy that they can carry off.

2.1 Calculation of Matrix element

We assume a sequential mechanism to describe the DCX reaction in ${}^4\text{He}(\pi^+, \pi^-)4p$. The operator for the pion DCX amplitude in the plane wave limit [15] can be written as

$$F_D(\mathbf{k}, \mathbf{k}', \mathbf{r}_1, \mathbf{r}_2) = \frac{1}{2\pi^2} \int d\mathbf{q} e^{-i\mathbf{k}'\cdot\mathbf{r}_2} f_2(\mathbf{q}, \mathbf{k}') \frac{e^{i\mathbf{q}\cdot(\mathbf{r}_2-\mathbf{r}_1)}}{q^2 - k_0^2} f_1(\mathbf{k}, \mathbf{q}) e^{i\mathbf{k}\cdot\mathbf{r}_1}, \quad (1)$$

where the pion-nucleon single charge exchange amplitude is represented as

$$f(\mathbf{k}, \mathbf{q}) = [\lambda_0 + \lambda_1 \mathbf{k} \cdot \mathbf{q} + i\lambda_f \sigma_2 \cdot (\mathbf{k} \times \mathbf{q})] v(q) v(k). \quad (2)$$

Here $\frac{1}{q^2 - k_0^2}$ is the pion propagator and $v(q)$ is the off-shell form factor taken here to be,

$$v(q) = \frac{\Lambda^2 + k^2}{\Lambda^2 + q^2}. \quad (3)$$

The quantity Λ (assumed here to be 4 fm^{-1}) is related to the range of the pion-nucleon interaction and the λ ’s are obtained from π -N phase shifts[16]. \mathbf{r}_1 and \mathbf{r}_2 denote the position vectors of the members of the struck nucleon pair. We first consider the double scattering to occur from two neutrons leading to a definite final state of 4 protons, as if it were an exclusive reaction. The density of these final states is then included to calculate the inclusive differential cross section. The matrix element for the reaction may be written as

$$M = \int d\mathbf{r}_1 d\mathbf{r}_2 d\mathbf{r}_3 d\mathbf{r}_4 \psi_{4p}(\mathbf{r}_1, \mathbf{r}_2, \mathbf{r}_3, \mathbf{r}_4) \langle S | F_D | 0 \rangle \psi_{He}(\mathbf{r}_1, \mathbf{r}_2, \mathbf{r}_3, \mathbf{r}_4) \quad (4)$$

where $\psi_{4p}(\mathbf{r}_1, \mathbf{r}_2, \mathbf{r}_3, \mathbf{r}_4)$ is the final state wave function for 4 protons. We assume that the four protons can be described by a product of plane wave states

$$\psi_{4p}(\mathbf{r}_1, \mathbf{r}_2, \mathbf{r}_3, \mathbf{r}_4) = \prod_{i=1}^4 e^{i\mathbf{p}_i \cdot \mathbf{r}_i} \quad (5)$$

$\psi_{He}(\mathbf{r})$ is the wave function of the initial state of ${}^4\text{He}$ which is taken here to have a Gaussian form:

$$\psi_{He}(\mathbf{r}_1, \mathbf{r}_2, \mathbf{r}_3, \mathbf{r}_4) = N e^{-\alpha(s_1^2 + s_2^2 + s_3^2 + s_4^2)}, \quad (6)$$

where $\mathbf{s}_i = \mathbf{r}_i - \mathbf{R}$, $\mathbf{R} = (\mathbf{r}_1 + \mathbf{r}_2 + \mathbf{r}_3 + \mathbf{r}_4)/4$, $N^2 = (\frac{\alpha}{\pi})^{\frac{9}{2}} \sqrt{8}$, $|0\rangle$ is the initial spin state for two neutrons in ${}^4\text{He}$ and $\langle S|$ is the final spin state of the struck pair. We assume a box normalization with unit volume.

For the spin independent piece of the pion-nucleon amplitude

$$M_0 = \frac{g(\mathbf{p}_3, \mathbf{p}_4)}{(2\pi^2)^{\frac{3}{2}}} \int d\mathbf{r} g(\mathbf{r}) e^{i(\frac{\mathbf{k}+\mathbf{k}'}{2}-\mathbf{p}) \cdot \mathbf{r}} e^{-\alpha r^2} \quad (7)$$

where

$$g(\mathbf{p}_3, \mathbf{p}_4) = 8^{\frac{1}{4}} e^{-\frac{(\mathbf{p}_3+\mathbf{p}_4)^2}{8\alpha}} e^{-\frac{(\mathbf{p}_3^2+\mathbf{p}_4^2)}{4\alpha}} \quad (8)$$

with $\alpha = \frac{p_f^2}{3}$ and

$$g(\mathbf{r}) = \int d\mathbf{q} \frac{e^{i\mathbf{q} \cdot \mathbf{r}}}{k_0^2 - q^2} f(\mathbf{q}, \mathbf{k}') f(\mathbf{k}, \mathbf{q}) \quad (9)$$

The differential cross section may be written as

$$\frac{d\sigma(\mathbf{k}, \mathbf{k}')}{d\Omega dk'} = \int |M|^2 d\mathbf{p}_3 d\mathbf{p}_4 d\Omega_p \frac{dp}{dk'} \quad (10)$$

The integral over the angles of the final relative pp momenta is done by standard numerical methods while the 6 dimensional integral over \mathbf{p}_3 and \mathbf{p}_4 is performed by Monte Carlo by sampling the last factor in Eq. 8.

For the more general case of a fully spin-dependent amplitude, we must consider amplitudes

$$F_{\sigma_{z1}, \sigma_{z2}}^{\sigma'_{z1}, \sigma'_{z2}} = \langle \sigma'_{z1}, \sigma'_{z2} | F_D | \sigma_{z1}, \sigma_{z2} \rangle \quad (11)$$

where F_D is the double scattering operator. The calculation of these amplitude is given in Appendix A.

2.2 Final State Interaction

The FSI is expected to play an important role in the low-energy region of the final nucleons (when the pion loses a small amount of energy) by increasing the value of matrix element. In this study, we introduce the effect of final state interaction among nucleons by taking into account of the interaction between the two protons in the pair which was produced from the two charge exchanges on the neutron pair. We calculate the correction coming from FSI by replacing the plane wave function for the active pair (the factor $e^{-i\mathbf{p} \cdot \mathbf{r}}$ in Eq. 7) by $\phi(\mathbf{p})$ which contains an interaction in the s-wave. The modified matrix element including the FSI is

$$M_{FSI} = \frac{g(\mathbf{p}_3, \mathbf{p}_4)}{(2\pi^2)^{\frac{3}{2}}} \int d\mathbf{r} g(\mathbf{r}) e^{i(\frac{\mathbf{k}+\mathbf{k}'}{2})\cdot\mathbf{r}} \phi(\mathbf{p}, \mathbf{r}) e^{-\alpha r^2} \quad (12)$$

where

$$\phi(\mathbf{p}, \mathbf{r}) = 4\pi \sum_{\ell, m} i^\ell \phi_\ell(p, r) Y_\ell^m(\mathbf{r}) Y_\ell^{m*}(\mathbf{p}). \quad (13)$$

Since we assume that the final pp interaction is important only in the relative s-wave

$$M_{FSI} = \frac{g(\mathbf{p}_3, \mathbf{p}_4)}{(2\pi^2)^{\frac{3}{2}}} \int d\mathbf{r} g(\mathbf{r}) e^{i(\frac{\mathbf{k}+\mathbf{k}'}{2})\cdot\mathbf{r}} [\phi_0(p, r) - j_0(pr)] e^{-\alpha r^2} + M_0. \quad (14)$$

We approximate $\phi_0(p, r)$ as

$$\phi_0(p, r) = \frac{\sin(pr + \delta_0) - \sin(\delta_0)e^{-\alpha_n r}}{pr}, \quad (15)$$

with $\alpha_n = 2m_\pi$. δ_0 is the s-wave phase shift which is calculated by using the pp version of the (modified) Malfliet-Tjon potential[17, 18].

The strength of the FSI can be expected to have a strong correlation with the outgoing energy of the pion and produce the greatest effect at high pion energies. One can see this qualitatively by considering a DCX reaction on two isolated neutrons at rest. Since the total momentum of the recoiling pair of protons is equal to the change in the momentum of the pion we can write the conservation of energy as

$$\omega - \omega' = \sqrt{4(p^2 + m^2) + (\mathbf{k} - \mathbf{k}')^2} - 2m. \quad (16)$$

Thus, for a fixed angle, the momentum, p , is a monotonic function of the final pion energy and the larger the final pion energy, the smaller is the relative momentum of the two final nucleons and the stronger the final state enhancement. For this reason we can expect the inclusion of FSI to increase the cross section at high outgoing pion energies with little effect at low pion energies. Figure 1 shows the result of the two-nucleon model with (solid line) and without (dashed line) final state interactions. It is seen that the strongest effect occurs at high final pion energy where a significant increase in cross section is observed.

3 Intranuclear Cascade Code

To get more a realistic picture of the reaction dynamics, we need to include the protons in the initial state in our calculation which we do by using an Intranuclear cascade (INC) code in which the pion moves through the nucleus with probabilities of different kinds of interaction until it escapes or is absorbed. For an overview see Appendix B.

Because the nucleons interact with classical potentials in this model, they can be deeply bound since there is no quantum constraint. To correct for this effect, these bound nucleons are freed and the binding energy removed from other particles. In the present case, bound nucleons were liberated with their final energy in their center of mass being a fixed number (20 MeV) equal to about what they would have from their Fermi motion. This value was varied

and little effect was seen. The energy needed to free the particles was taken from the pion which is probably the right particle in many, but not all, cases. This feature is perhaps the most unrealistic aspect of the current INC code. This defect could perhaps be corrected using the method of Wilets et al. [19] but such a correction is beyond the scope of the present work.

3.1 Final State Interactions

The INC technique calculates the DCX cross section by following the classical motion of the pion through the nucleus. While there are interactions among all of the nucleons through potentials, as described in Appendix B, they are not of the quantum mechanical nature that was included in the two-nucleon model when FSI was treated. This QM correction is included in the INC by the use of a weighting factor for each event. When a DCX event takes place, all of the coordinates of the pion and the nucleons are known so that the matrix elements M_0 and M_{FSI} can be evaluated. Since the event includes no QM FSI, one can correct the probability of its occurrence by including a weight which is equal to the ratio of the squares of these two matrix elements.

3.2 Pion Production

The aim is to model pion production, given a knowledge of pion production from a nucleon in free space. The total cross section for pion production from a free nucleon can be computed from the inelasticity in the phase shifts[16] since, for the moderate energies treated here, the $(\pi, 2\pi)$ reaction is the sole significant contributor to the inelasticity.

Once it has been decided that a pion production event would take place in free space (based on the ratio of the pion production cross section to the total cross section), the distribution of the three-particle final state (two pions and one nucleon) in energy and angle must be modeled. To compute these functions the current relevant data are inadequate, so we have used two-step models. One possible model is that in which a Δ and a pion are produced with the Δ decaying to produce the second pion. This mechanism may indeed play a role. A second mechanism believed to be important just above threshold, would produce a “ σ ” meson and then have it decay into two pions. The early data favors this mechanism, as does the fact that the production of an isospin zero pion pair is dominant.

Here we use the “ σ ” mechanism only in the sense that the pion-nucleon system is converted into a two-pion plus nucleon system (assumed isotropic in the original πN center of mass) and then the two pion subsystem is allowed to decay (again isotropically). To model the apportionment of energy between the nucleon and the two-pion system we assume a distribution of the two-pion invariant mass proportional to $Q(Q_{max} - Q)$ where Q is the momentum of one of the pions in their center of mass. Once these variables have been chosen, the momentum of the remaining nucleon is known. A Pauli blocking test (requiring that the nucleon must not have less energy in the final state than in the initial state) is applied, resulting in a significant fraction of the possible production events being disallowed.

The total pion production cross section calculated at 240 MeV is 116 μb . Since the production cross section from a single free nucleon is about 600 μb , considerably less than the maximum possible cross section is obtained. This reduction is very likely largely due to the two protons which “shield” the neutrons from which production takes place.

3.3 Pauli Blocking

The effect of Pauli Blocking becomes important at low energy. If there is little energy loss by the pion the energy of the 4 protons will be small. In this case there will be strong cancellation among in the Pauli terms as was discussed by Ref. [7]. Hence, we expect a reduction in the cross section due the Pauli principle. The effect of Paul blocking is taken into account in this study by using a weighting factor which consists of an incoherent summation of the squares of the expressions in Eqs. 17 and 18 (taken from Ref [7]).

$$A_1 = \frac{1}{\sqrt{24}}[2A(1234) + 2A(2134) - A(1423) - A(1324) - A(24321) - A(2341) - A(3214) - A(4213) - A(3124) - A(4123) + 2A(3412) + 2A(4321)] \quad (17)$$

$$A_2 = \frac{1}{\sqrt{8}}[A(1324) - A(1423) + A(2431) - A(2341) - A(3214) + A(4213)A(3124) - A(4123)] \quad (18)$$

where

$$A(abcd) = e^{i(\mathbf{p}_a \cdot \mathbf{r}_1 + \mathbf{p}_b \cdot \mathbf{r}_2 + \mathbf{p}_c \cdot \mathbf{r}_3 + \mathbf{p}_d \cdot \mathbf{r}_4)} \quad (19)$$

The momenta in the first two positions correspond to those associated with the two nucleons on which the charge exchange occurs. Tests including this effect showed that it was very small at the energies considered here and this weight was not normally included in the calculation.

4 Discussion

We performed calculations for doubly differential cross sections by two methods, the first being described in Section 2 with the results shown in Fig. 1. Our results at small angles clearly show the effect of the FSI which is around 30% at the peak at 25 degrees.

It is clear from this figure that the two-nucleon model overestimates the absolute cross section in the region of the high-energy peak. The discrepancy could be due to the ignoring of scattering from the two ‘‘spectator’’ protons in our calculation.

Figure 2 shows a comparison of the two models under the same conditions (i.e. only the two neutrons are included in the scattering in the INC). The same basic physics is present in the two models (one classical and one quantum) which are seen to give very similar results at 240 MeV.

Figure 3 shows the effect of including the two initial protons at 270 MeV. It is seen that the cross section is considerably diminished. The two protons are very effective in shielding the neutrons from the incident pion.

Figure 4 shows the results with and without the FSI. It is seen that its inclusion by using a calculated weight in the INC is very similar to the direct calculation in the two-nucleon model (see Fig. 1), the principal effect being at forward angles and high-energy outgoing pions. The shape of the high energy peak is influenced by the effect of the FSI.

These effects modify the cross section by up to a factor of 3. Figure 5 shows the progression from the case with only 2 nucleons to the addition of the protons (without true absorption) to the addition of true absorption.

Figure 6 shows the effect of FSI at 180 MeV. Our calculation overestimates the cross section but less than the other calculations [9, 14]. That could be due to the fact that 180 MeV is very close to the P_{33} resonance peak, so that we expect a great deal of absorption to occur. It is also possible that the INC does not give good results at the resonance peak because there is a larger degree of coherence, not taken into account by the classical INC.

While the full calculations (solid curves in Figs. 4 and 5) give good results for the high-energy peak, the low-energy peak is underestimated by about a factor of two at forward angles. Figures 7 and 8 show the effect of inclusion of pion production. Pion production complements the DCX channel at pion incident energies of 240 and 270 MeV, and influences the shape and value of the spectra in the region of the low energy peak. Vicente *et al.*[20] found that the pion production enhances the strength of the DCX cross section by 15% at 240 MeV and 30 % at 270 MeV in $^{16}\text{O}(\pi^+, \pi^-)X$. This same mechanism apparently explains the missing strength at the low energy peak at 270 MeV and 240 MeV in the present case.

A measurement of pion production from ^3He was made in Ref. [10]. In this study negative pions were detected with a incoming π^+ beam. Since there is no double charge exchange possible, the π^- mesons must arise from pion production. Since there is only a single neutron in ^3He , whereas in ^4He there are two and since the blocking effects of the two protons should be about the same in the two cases, we expect the production in ^4He to be about twice that in ^3He . In Fig. 7 we show the data from Ref. [10] multiplied by a factor of two. The agreement with this data under this assumption is satisfactory.

In regard to the possible forward-backward explanation of the two peaks, we note first that the effect is being observed in the laboratory. Even if the single charge exchange angular distribution remained forward-backward symmetric in the center of mass, it would become more forward peaked in the lab as the energy increases which would lead to the high energy peak becoming increasingly dominant. In fact the single charge exchange angular distribution becomes more forward peaked in the center of mass as well. These two effects lead one to expect a decreasing low-energy peak with rising beam energy since it is supposed to arise from the back scattering part of the angular distribution. The data show the opposite effect with the low-energy peak growing with respect to the high-energy one with increasing energy. This observation is naturally explained if pion production is important since its contribution rises with energy.

Figure 9 shows the integrated total DCX cross section with the INC compared with data.

5 Conclusion

In this paper, we have presented calculations of the double charge exchange cross section for reaction $^4\text{He}(\pi^+, \pi^-)2\text{p}$ by using a sequential mechanism and an INC model. The consideration of FSI in our calculation enhances the high energy peak at small angles by 30 % leading to good agreement with experimental data. The missing cross section strength in the low energy peak in our calculation at energies 240 and 270 MeV is naturally explained by pion production.

We note that there is a discrepancy between theory and experiment in regard to the shape

of the 180 MeV data. While inclusive pion production gives only a very small contribution (one is only about 5 MeV above threshold) a significant contribution can come from the production leading to ${}^3\text{He}$ plus a proton. The threshold for this reaction is about 167 MeV. The calculation of this cross section is beyond the scope of the techniques used in the present paper.

We wish to thank Mark Yuly for supplying the numerical values for the production cross section on ${}^3\text{He}$ from Ref. [10]. This work was supported by the National Science Foundation and the Jordan University of Science and Technology.

A Spin Dependence

To include spin in the calculation, it is preferable to rewrite the pion-nucleon scattering amplitude in a slightly different form.

By using the relations

$$\hat{\mathbf{q}} \cdot \hat{\mathbf{q}}' = -\frac{4\pi}{\sqrt{3}} \sum_{m,m'} C_{1,1,0}^{m,m',0} Y_1^m(\hat{\mathbf{q}}) Y_1^{m'}(\hat{\mathbf{q}}') \quad (20)$$

and

$$\sigma \cdot \hat{\mathbf{q}} \times \hat{\mathbf{q}}' = \frac{8\pi i}{3\sqrt{2}} \sum_{m,m',M} C_{1,1,1}^{m,m',M} \sigma^{-M} Y_1^m(\hat{\mathbf{q}}) Y_1^{m'}(\hat{\mathbf{q}}') \quad (21)$$

we can then express the πN amplitude as

$$\mathbf{f}(\mathbf{q}, \mathbf{q}') = \sum_{\beta=0,1,2} \left(\frac{1}{\sqrt{3}}\right)^\beta \mathbf{D}_\beta(\mathbf{i}) \mathbf{q}^\alpha \mathbf{q}'^\alpha \mathbf{v}_\alpha(\mathbf{q}) \mathbf{v}_\alpha(\mathbf{q}') \sum_{\mathbf{m}, \mathbf{m}', \mathbf{M}} \mathbf{C}_{\alpha, \alpha, \gamma}^{\mathbf{m}, \mathbf{m}', \mathbf{M}} \mathbf{t}_\gamma^{-\mathbf{M}}(\mathbf{i}) \mathbf{Y}_\alpha^{\mathbf{m}}(\hat{\mathbf{q}}) \mathbf{Y}_\alpha^{\mathbf{m}'}(\hat{\mathbf{q}}') \quad (22)$$

where α , β and γ are related by the following table.

β	α	γ
0	0	0
1	1	0
2	1	1

The matrices t_0 and t_1^μ are defined by

$$t_0^0 = \begin{pmatrix} 1 & 0 \\ 0 & 1 \end{pmatrix}$$

$$t_1^0 = \sigma^0 = \sigma_z; \quad t_1^1 = \sigma^1 = -\frac{1}{\sqrt{2}}(\sigma_x + i\sigma_y); \quad t_1^{-1} = \sigma^{-1} = \frac{1}{\sqrt{2}}(\sigma_x - i\sigma_y)$$

and

$$D_0(i) = 4\pi\lambda_0(i); \quad D_1(i) = \frac{4\pi}{\sqrt{3}}\lambda_1(i); \quad D_2(i) = \frac{8\pi i}{\sqrt{6}}\lambda_2(i)$$

The operator in spin space for the double scattering will then be given by

$$\begin{aligned}
\mathbf{F}_D(\mathbf{k}, \mathbf{k}') &= \sum_{\beta_1, \beta_2} D_{\beta_1}(1) D_{\beta_2}(2) k^{\alpha_1} k'^{\alpha_2} Y_{\alpha_1}^{m_1}(\hat{\mathbf{k}}_1) Y_{\alpha_2}^{m_2'}(\hat{\mathbf{k}}_2) \times \\
&\left(\frac{1}{\sqrt{3}}\right)^{\gamma_1 + \gamma_2} C_{\alpha_1, \alpha_1, \gamma_1}^{m_1, m_1', M_1} C_{\alpha_2, \alpha_2, \gamma_2}^{m_2, m_2', M_2} t_{\gamma_1}^{-M_1}(1) t_{\gamma_2}^{-M_2}(2) \\
&\times A_{\alpha_1, \alpha_2}^{m_1', m_2}(\mathbf{k}_0, \mathbf{r})
\end{aligned} \tag{23}$$

where

$$A_{\alpha_1 \alpha_2}^{m_1' m_2}(k_0, r) = \int q^{\alpha_1 + \alpha_2} Y_{\alpha_1}^{m_1}(\hat{\mathbf{q}}) Y_{\alpha_2}^{m_2'}(\hat{\mathbf{q}}) \left(\frac{\alpha^2 + k_0^2}{\alpha^2 + q^2} \right)^2 \frac{e^{i\mathbf{q}\cdot\mathbf{r}}}{(k_0^2 - q^2)} d\mathbf{q}$$

We are now ready to calculate the matrix elements of this operator in spin space. Using

$$\langle \sigma' | t_1^{-M} | \sigma \rangle = -\sqrt{3} C_{\frac{1}{2}, 1, \frac{1}{2}}^{\sigma', -M, \sigma} \tag{24}$$

we can write

$$\begin{aligned}
&\langle \sigma_1', \sigma_2' | \mathbf{F}_D(\mathbf{k}, \mathbf{k}') | \sigma_1, \sigma_2 \rangle \equiv \mathbf{F}_{D_{\sigma_1, \sigma_2}}^{\sigma_1', \sigma_2'}(\mathbf{k}, \mathbf{k}') \\
&= \sum_{\beta_1, \beta_2} (-1)^{M_1 + M_2} D_{\beta_1}(1) D_{\beta_2}(2) \mathbf{k}^{\alpha_1} \mathbf{k}'^{\alpha_2} Y_{\alpha_1}^{m_1}(\hat{\mathbf{k}}) Y_{\alpha_2}^{m_2'}(\hat{\mathbf{k}}') \times \\
&C_{\alpha_1, \alpha_1, \gamma_1}^{m_1, m_1', M_1} C_{\alpha_2, \alpha_2, \gamma_2}^{m_2, m_2', M_2} C_{\frac{1}{2}, \gamma_1, \frac{1}{2}}^{\sigma_1, -M_1, \sigma_1'} C_{\frac{1}{2}, \gamma_2, \frac{1}{2}}^{\sigma_2, -M_2, \sigma_2'} A_{\alpha_1, \alpha_2}^{m_1', m_2}(\mathbf{k}_0, \mathbf{r})
\end{aligned} \tag{25}$$

B The Intranuclear Cascade

The present code was originally developed to treat moderate-energy antiproton annihilation in nuclei and has been applied to that end several times [23, 24, 25, 26, 27, 28]. The annihilation of an antiproton leads to pions (or at least it is so treated by the code) and so the history of pions in the energy range below and of the order of 1 GeV are essential to the calculation of energy deposition. It has had considerable success in predicting the rapidity distributions of strange particles produced in antiproton reactions[25]. The question of pion absorption and comparison with data has been addressed [29] and the code has been used for the comparison with inclusive data in work by Zumbro *et al.*[30].

The initial bombarding projectile is started with appropriate initial momentum toward a circle which is large enough to contain the projected density of the target nucleus. A fraction of the beam particles (usually about one half) pass without interacting and cross sections are computed as the fraction of the reactions of interest which occur multiplied by the area of this disk.

B.1 Treatment of Nucleons

The heart of the code is the construction of a model nuclear system with as many characteristics of a “real” nucleus as possible. The code exists in several versions according to the reaction being investigated and the detail required.

B.1.1 Version I: The Woods-Saxon Potential

In this original model the nucleon-nucleon interaction is thought of as being made up of two parts: 1) a long range interaction (one pion exchange) and 2) a short-range part (heavy meson exchange, quark interaction, etc.).

The average of the long-range part is represented by a potential with a Woods-Saxon shape. The parameters of the well are chosen so that the particle distribution that results from motion in this well represents the measured proton densities in nuclei.

Each nucleon has a designated binding energy specified in the input data. For a given binding energy there is a point at the edge of the well where the potential is equal to the binding energy and hence the kinetic energy is zero. For each particle a limiting radius, R_x , is chosen as that value of the radius and a set of position coordinates are chosen uniformly distributed within a sphere of radius R_x . Once the position for a given nucleon is established, its potential energy can be calculated and, using the specified binding energy, the kinetic energy and hence the magnitude of the momentum, can be obtained. The directions of the momenta are chosen randomly in an isotropic manner. Since each particle is moving in a conservative potential well it will maintain the same total (binding) energy throughout its motion unless disturbed by an outside agent.

The short-range part of the nucleon-nucleon interaction is represented by a scattering cross section.

B.1.2 Version II: Inter-nucleon Potentials with Fixed Well

In this version the potential well is generated by the superposition of semi-realistic nucleon-nucleon potentials due to the nucleons themselves, those by Malfliet and Tjon [17, 18].

If V_i is the potential seen by the i^{th} nucleon at position \mathbf{r}_i then

$$V_i = \frac{1}{2} \sum_{i \neq j} V_{ij}(|\mathbf{r}_i - \mathbf{r}_j|) \quad (26)$$

where the subscript ij on V is to label whether the interaction is np or pp (nn). For the technique of creating the initial nucleus see section B.3.

If we wish to guarantee that the nucleus remains in the ground state (i.e. with each nucleon keeping its assigned binding energy) we can fix the wells to those generated by the originally chosen nucleons with each nucleon moving in its own fixed well, even though the other nucleons which created this potential have moved to other positions as the time evolution progresses. Since the movement of non-struck nucleons is small, the actual wells should not be very different from these fixed wells. The reason for wanting to keep the fixed wells is to maintain the quantum condition that the nucleus remain intact with the same “quantized” states unless acted upon by an external force. As before, the nucleons can collide with a probability computed from a cross section entered as data. Note that this is necessary since the nucleons cannot exchange energy except by this mechanism. A nucleon may scatter from another nucleon’s initial position but it simply bounces off of the potential and the nucleon “struck” knows nothing of the interaction.

One inconvenient point which is especially bothersome for light nuclei is that a single nucleon can be left bound in the phantom potential well. For example for ${}^4\text{He}$ if, in π^+

absorption, three protons are removed, the remaining neutron is still bound in the well (if it is not specifically struck by the incident pion or one of the leaving nucleons) and is left with a negative energy when it should have a positive energy distribution (presumably related to its Fermi momentum).

It is this version which was used for the inclusive measurements by Zumbro *et al.* [30].

B.1.3 Version III: Inter-nucleon Potentials with a Changing Well

In this case the calculation of the potential wells follow the nucleons as they move. In some sense this is the most realistic of all the models. It has problems, however. As in any classical model the particles can evaporate from the system. If the nucleus falls apart rapidly the density at which the reaction takes place may not be correct, even though the initial nucleus is originally thrown with an acceptable density. To minimize this problem the nucleons do not begin to move until there is a first interaction of the projectile with one of them. Note that a typical nuclear reaction takes place on the order of a few fm/c. Thus, while the nucleus is decreasing in density as a function of time, the problem is not very serious.

B.2 Interaction of the Projectile with the Nucleons

The next step is to allow the projectile to propagate through the nucleus and interact with the nucleons. Only pions will be treated in the present discussion. Kaons, η 's and other mesons are also propagated by similar techniques. Immediately after moving the nucleons one time step the meson multiple scattering subroutine is entered. This subroutine moves the pion (or pions) one time step, taking into account the possibility that it can elastically scatter, charge exchange, be absorbed on a nucleon pair or produce one or more additional pions.

For each pion the following steps are carried out.

The distance from the pion to each nucleon is computed and compared with the value of R derived from the equation

$$\sigma_{max} = \pi R^2 \tag{27}$$

where σ_{max} is the maximum pion-nucleon total cross section (that at the 33 resonance). If the distance is greater than R the index of the loop passes on to the next nucleon. The total cross sections used for comparison are π^0 cross sections, or in other words, the average of π^+ and π^- cross sections. A weight is carried for the event which is the ratio of the true total cross section to the π^0 total.

If the distance is less than R then the possibility that an interaction might take place is pursued. From the momenta of the pion and the nucleon the effective laboratory momentum for the pion is computed, i.e. the value the pion would have (for the same center of mass energy) if the nucleon were at rest. This is done because c.m. cross sections are tabulated as a function of P_{lab} . The distance from the pion to the nucleon is then compared with a length, R , obtained from $\sigma_T(P_{lab}) = \pi R^2$ where σ_T is tabulated in a vector indexed by P_{lab} . If the distance is greater than this number then there is no interaction with that nucleon.

When a case is found that the distance to the nucleon is less than R then a weight for the event is computed from the ratio of cross sections and one of a series of branchings is selected according to conservation laws and the appropriate probability.

First, the possibility of pion absorption is explored. In order for a pion to be absorbed it must have interacted previously with at least one nucleon and absorption must be possible (charge conservation). If those two conditions are met, then a random number is compared with an input parameter, P_{abs} , to determine if an absorption will take place.

If the pion is absorbed then the total energy of the pion is converted into momentum added to the current and previous nucleon in such a way that the sum of the additional momenta are zero (they are equal and opposite) and along the direction of the trajectory of the pion traveling between the two nucleons, i.e. parallel to the current pion momentum. If \mathbf{p}_π is the current value of the pion momentum then the current nucleon will receive

$$\mathbf{P} + \frac{\mathbf{P}_\pi}{2} \equiv \alpha \mathbf{p}_\pi \quad (28)$$

and the previous nucleon

$$-\mathbf{P} + \frac{\mathbf{P}_\pi}{2} \equiv \beta \mathbf{p}_\pi. \quad (29)$$

To conserve energy we have (non-relativistically)

$$\frac{(\mathbf{P}_1 + \alpha \mathbf{p}_\pi)^2}{2m} + \frac{(\mathbf{P}_2 + \beta \mathbf{p}_\pi)^2}{2m} = \frac{P_1^2}{2m} + \frac{P_2^2}{2m} + \omega \quad (30)$$

Where 1 (say) is associated with the current nucleon and 2 with the previous one. Solving for α and β the momentum \mathbf{P} can be found. The direction of \mathbf{p}_π relative to the incident beam direction (in the case of only two nucleons) approximately follows a p-wave distribution from the previous elastic scattering. The direction of this large momentum dominates the angular distribution and tends to give a reasonably good representation of πd absorption.

If pion absorption does not take place then the possibilities of pion production (if energy conservation permits), charge exchange (if charge conservation permits) or elastic scattering are chosen according to the ratio of the relevant cross sections to the total.

If pion production does not take place then charge exchange or elastic scattering occur. In this case a table of Legendre polynomial coefficients are used (from a data table) to select an angular distribution for the final two particles. If the scattering or charge exchange leads to a nucleon whose energy is not greater than its initial value by the amount of the Pauli blocking energy the scattering is not allowed.

B.3 Technique for creating a Nucleus with correlations

The procedure starts from the point of view of the shell model. The full Hamiltonian can be written as

$$\sum_i T_i + \frac{1}{2} \sum_{j \neq i} V_{ij}(\mathbf{r}_i - \mathbf{r}_j) = E \quad (31)$$

This equation can be regarded as a classical or operator relationship.

In the spirit of the shell model it is natural to write the total energy as the sum of single-particle energies $E = \sum_i E_i$ and make the association

$$T_i + \frac{1}{2} \sum_j V_{ij}(\mathbf{r}_i - \mathbf{r}_j) = E_i \quad (32)$$

for each particle. Certainly this is not necessary but it is sufficient to satisfy the original equation and it allows us to associate an energy with each particle. These equations may be regarded as operator equations for the Schrödinger equation or simply classical energy conservation equations. A significant difference is that in the quantum case the kinetic energy symbols mean derivative operators and in the classical case they are non-negative quantities. In the quantum case they lead to negative multipliers of the wave function only in the case of tunneling. Since tunneling is a small probability we make the approximation that the kinetic energies should always be positive. In any event, we are forced to require that the kinetic energies be non-negative for the construction of the nucleus since it is to be used in a classical simulation.

The resulting algorithm can be described as follows:

1) All of the particles are assigned a value of binding energy in the shell model sense. As an example, for ^{12}C , there might be 4 particles with a binding energy suitable for the s-shell and 8 particles with a binding energy in the p-shell. The sum of these binding energies should be equal to the total binding energy of the nucleus.

2) Each shell is assigned a sphere with some defined radius. This radius parameter allows a fine tuning of the radius for each shell to be obtained. If this radius is taken too small the nucleus will be compressed. If it is taken too large time will be wasted in attempting to create impossible configurations. In general it should be taken of the order of the effective square well radius of a given shell.

3) A nucleon-nucleon potential is assigned to each particle pair. In general this is defined between particle types (nn and pp or np).

4) The actual creation of the nucleus is begun with the throwing of a random uniform distribution of particles within the spheres defined above.

5) The calculation of each kinetic energy is made using the positions of the nucleons to calculate the potential energy and subtracting it from the individual binding energies. If any kinetic energy is negative then the complete re-throw of the nucleus is started again with step 4. If all kinetic energies are non-negative then the proposed nucleus is possibly viable. Note that the particles cannot be very close or the repulsive potential will make some kinetic energy negative nor can they be too far apart for the same reason.

6) Now the magnitudes of the momenta are calculated from the kinetic energies and the directions are thrown in a random uniform manner. This process will lead to a nucleus with a non-zero total momentum.

7) The total momentum of the nucleus is calculated by vectorially adding the individual momenta. If the magnitude exceeds a set limit, the angles of the momentum vectors are thrown again in an attempt to make the sum less than the limit returning to step 6. Since it is possible that no combination of angles will lead to a total momentum less than the prescribed limit, after some fixed number of tries (typically 300) the entire nucleus is re-thrown by returning to step 4.

8) $1/A$ of the total momentum is subtracted from each nucleon thus putting the nucleus at rest. This procedure does not leave the binding energy unchanged but if the limit on the total momentum is small the error on the binding energy is also small. For example, it was found that if the total momentum is restricted in step 7 to be less than 40 MeV/c then the maximum error in the binding energy was observed to be less than 0.2 MeV (out of 28 MeV) for ^4He .

References

- [1] N. Auerbach, W. R. Gibbs, Joseph N. Ginocchio and W. B. Kaufmann, *Phys. Rev. C* **38**, 1277 (1988); W. R. Gibbs, J. N. Ginocchio and N. Auerbach, *Comments in Nuclear and Particle Physics*, **20**,141 (1991).
- [2] Mutazz Nuseirat, M. Elghossain, M. A. K. Lodhi, W. R. Gibbs and W. B. Kaufmann, *Phys. Rev. C* **58**, 2292(1998)
- [3] H. C. Wu and W. R. Gibbs, *Phys. Rev. C* **62**, 044614 (2000)
- [4] F. Becker and C. Schmit, *Nucl. Phys.* **B18**,607(1970).
- [5] J. F. Germond and C. Wilkin, *Lett. Nuovo Cimento* **13**,605(1975).
- [6] J. B. Jeanneret, M. Bogdanski, and E. Jeannet, *Nucl. Phys.* **A350**, 345(1980).
- [7] W. R. Gibbs, A.T. Hess, and G. J. Stephenson, *Phys. Rev. C* **15**,1384(1977).
- [8] J. Grater *et al.*, *Phys. Rev. C* **58**,1576(1998).
- [9] E. R. Kinney, J. L. Matthews, P. A. M. Gram, D. W. Mac Arthur, E. Piassetzky, G. A. Rebka, Jr., D. A. Roberts, *Phys. Rev. Lett.* **57**,3152(1986).
- [10] M. Yuly *et al.*, *Phys. Rev. C* **55**,1848(1997)
- [11] S. A. Wood, Los Alamos National Laboratory Report No. LA-9932-T,1983.
- [12] S. A. Wood, J. L. Matthews, E. R. Kinney, *et al.* *Phys. Rev. C* **46**,1903(1992)
- [13] J. Van Loon, Masters Dissertation, Free University, Amsterdam (unpublished), 1985
- [14] A. V. Kulkarni, Ph.D. Thesis, University of Wyoming (1994)
- [15] W. R. Gibbs, M. Elghossain and W. B. Kaufmann, *Phys. Rev. C* **48**, 1546 (1993).
- [16] Center for Nuclear Studies [SAID Program] <http://gwdac.phys.gwu.edu/>
- [17] R. A. Malfiet and J. A. Tjon, *Nucl. Phys.* **A127**, 161(1969)
- [18] W. R. Gibbs, *Computation in Modern Physics*, (World Scientific, Singapore, 1999).
- [19] L. Wilets, E. M. Henley, M. Kraft and A. D. Mackellar, *Nucl. Phys. A* **282**, 341(1977)
- [20] M. J. Vicente, E. Oset, L. L. Salcedo, and C. Garcia Recio, *Phys. Rev. C* **39**, 209,(1989).
- [21] L. V. Falomkin *et al.*, *Nuovo Cimento A*, **22**,333(1974).
- [22] A. Stetz *et al.*, *Phys. Rev. Lett.* **47**,782(1981)
- [23] S. Ahmad *et al.*, "Proceedings of the Fourth Biennial Conference on Low Energy Antiproton Physics", Dinkelsbühl, Germany, 27 Aug., 1996 *Nucl. Phys. B Sup.* **56A**, 118(1997)
- [24] W. R. Gibbs, Proc. of the "Intersections Between Particle and Nuclear Physics", Lake Louise, Canada 1986 AIP Conference Proceedings 150, p. 505
- [25] W. R. Gibbs and J. W. Kruk, *Phys. Lett.* **317B**, 237(1990); *Z. Phys.* **C46**, S45(1990)

- [26] W. R. Gibbs, Proc. of the “First Fermilab Workshop on Low-Energy Antiproton Physics” April 10-12, 1986, page 355
- [27] W. R. Gibbs and D. Strottman, Proc. of the “International Conference on Antinucleon- and Nucleon-Nucleon Interactions”, Telluride, CO March 18-21, 1985. Plenum Press, New York
- [28] D. Strottman and W. R. Gibbs, *Phys. Lett.* B149, 288 (1984)
- [29] W. R. Gibbs and W. B. Kaufmann, Proc. of LAMPF Workshop on “Pion-nucleus Physics: Future Directions and New Facilities at LAMPF”, AIP Conference Proceedings 163, p. 279 **B231**, 6 (1989)
- [30] J. D. Zumbro, C. L. Morris, J. A. McGill, S. J. Seestrom, R. M. Whitton, C. M. Riedel-Edwards, A. L. Williams, M. Braunstein, M. Kohler, B. Kriss, S. Hoibraten, R. J. Peterson, J. Ouyang, J. E. Wise, and W. R. Gibbs, *Phys. Rev. Lett.* 71, 1796(1993)

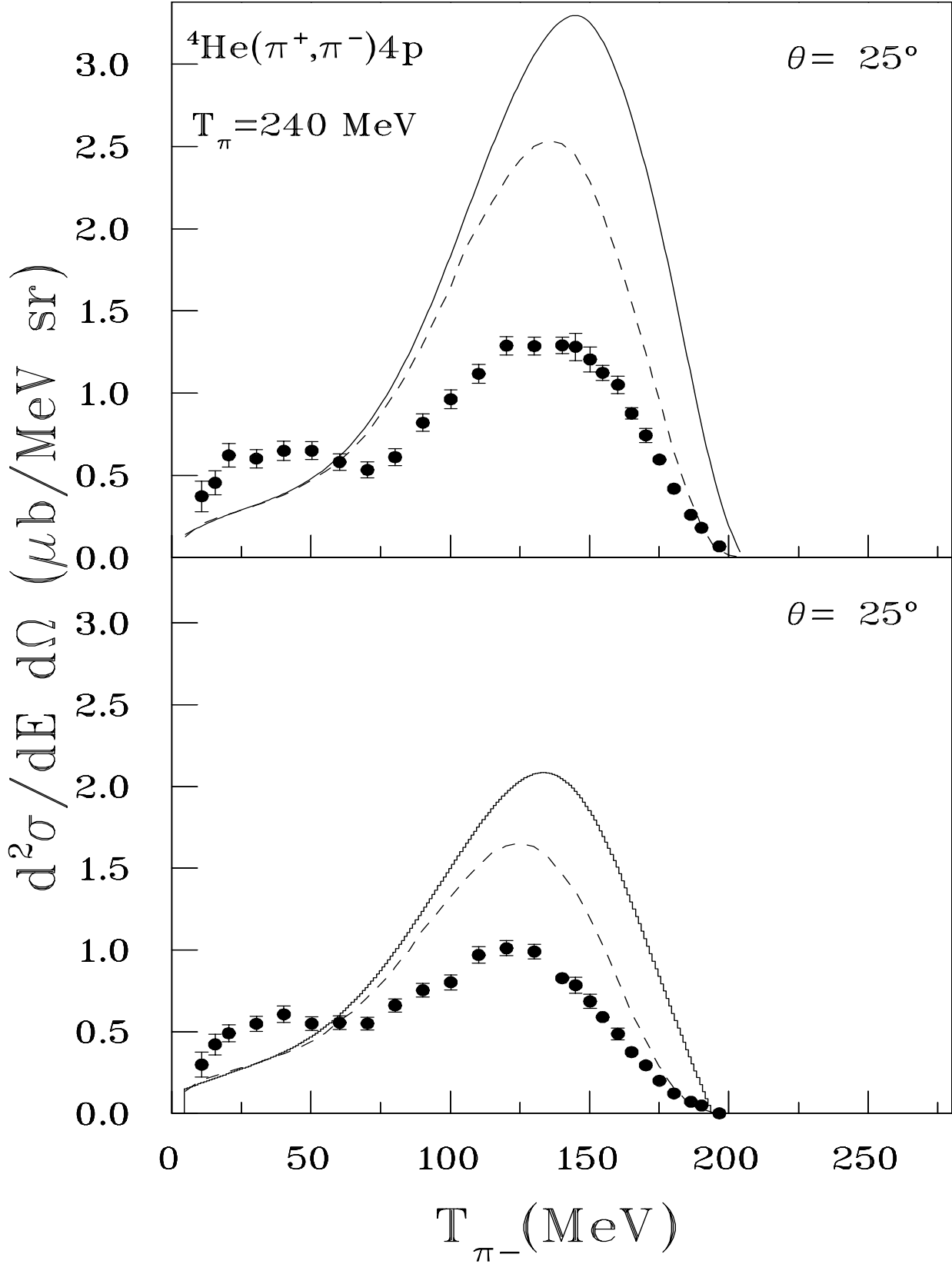


Figure 1: Results of the two-nucleon model without (dashed line) and with (solid line) final state interaction FSI.

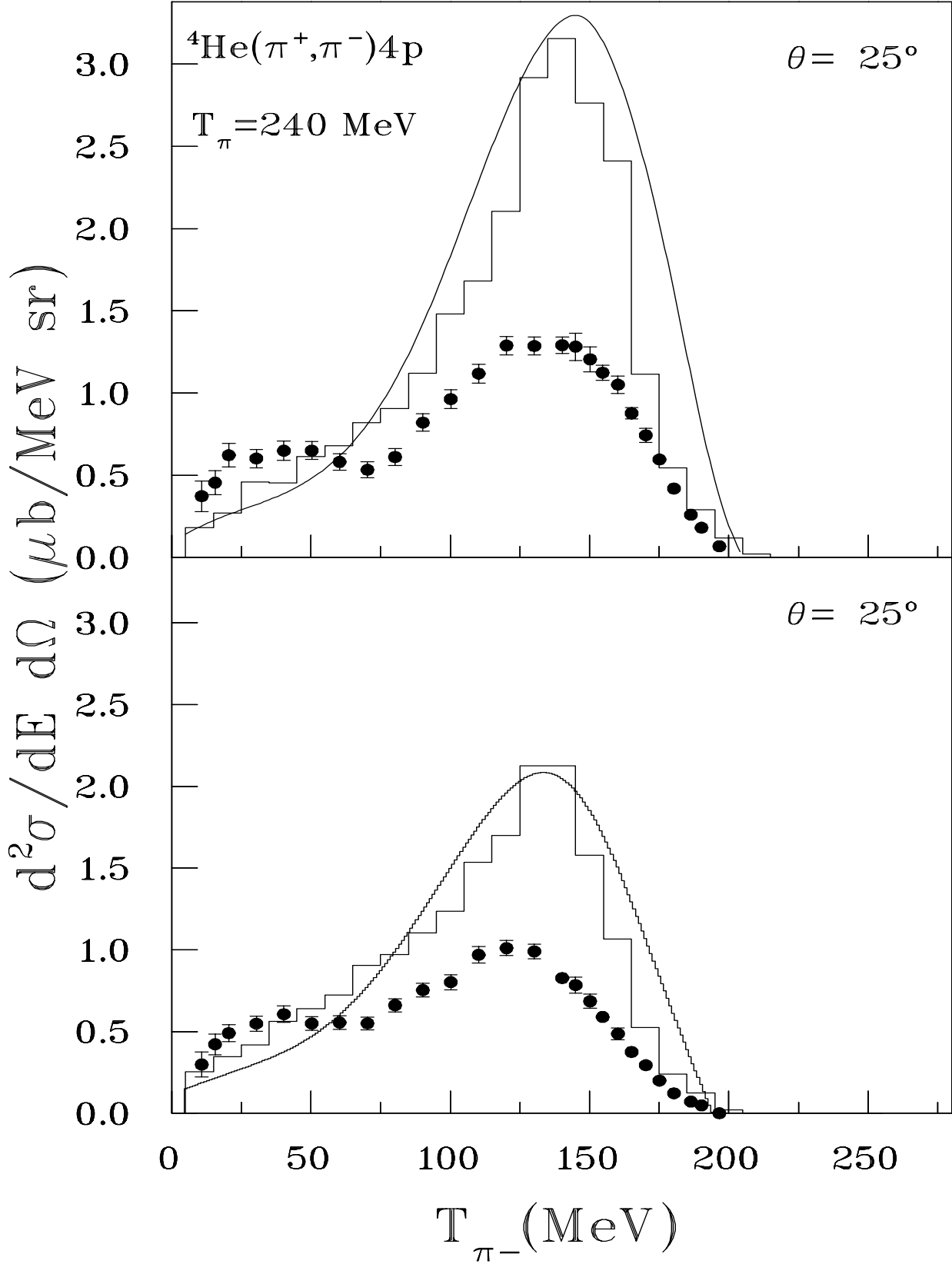


Figure 2: Comparison of the INC with only two nucleons (neutrons) active (histogram) with the two-nucleon model (solid line).

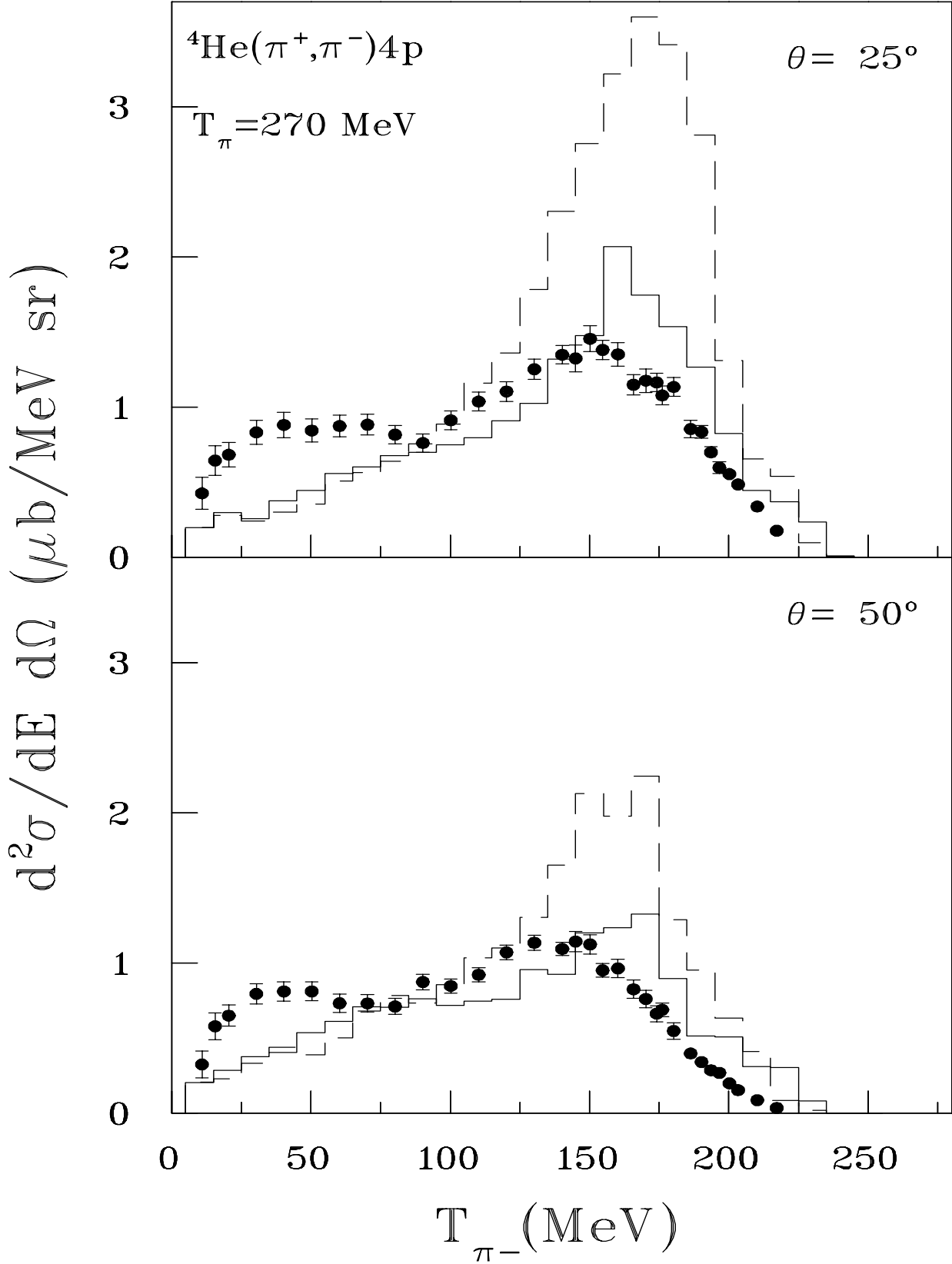


Figure 3: The results of INC model at incident energy 270 MeV with only the two neutrons (dashed histogram) and four nucleons (solid line histogram).

$$d^2\sigma/dE d\Omega \text{ (}\mu\text{b/MeV sr)}$$

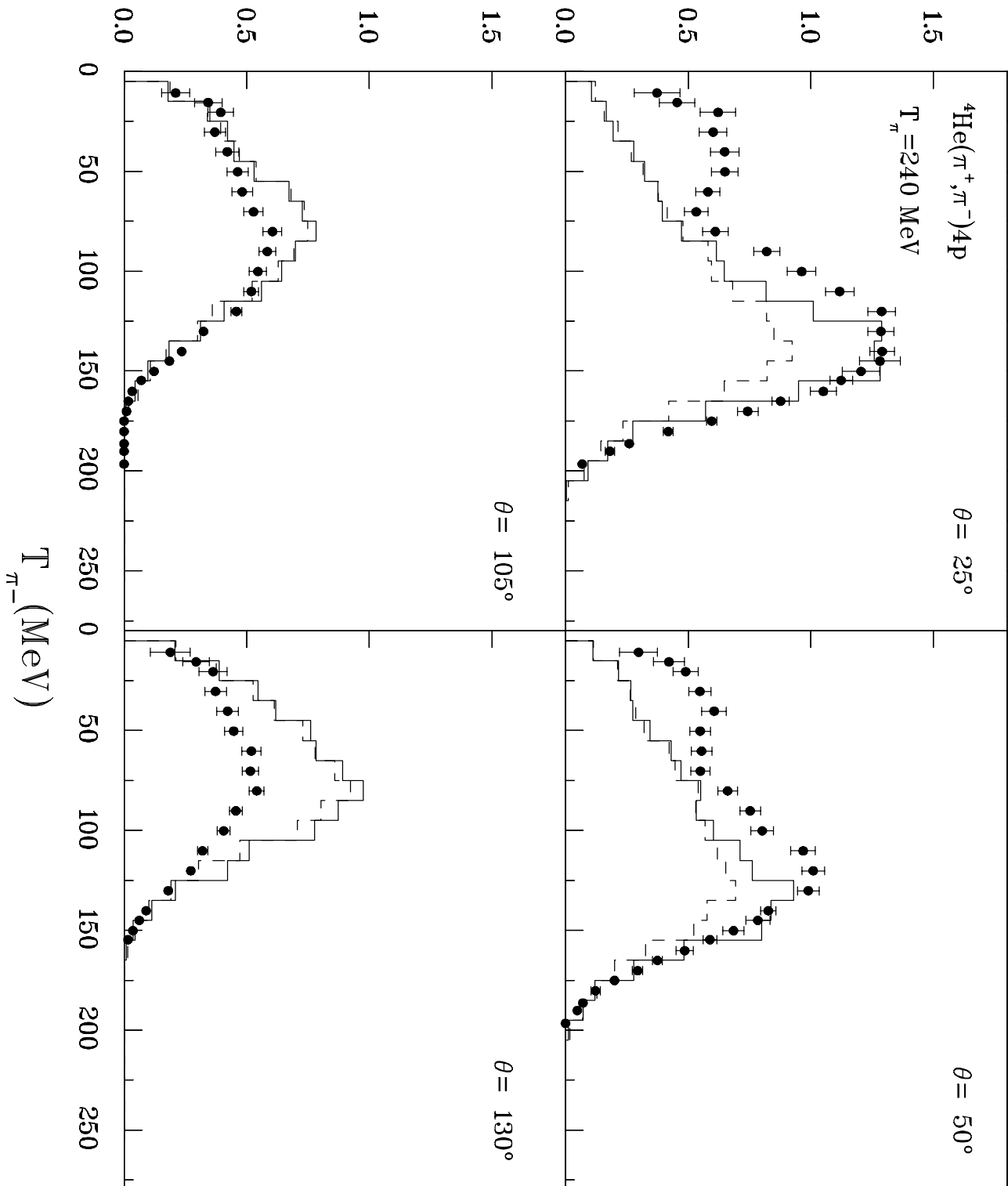


Figure 4: The results of doubly differential cross section for the reaction ${}^4\text{He}(\pi^+, \pi^-)4\text{p}$ at incident pion energy of 240 MeV. The calculation of the solid histogram includes FSI and the dashed line histogram does not (absorption is included in both).

$d^2\sigma/dE d\Omega$ ($\mu\text{b}/\text{MeV sr}$)

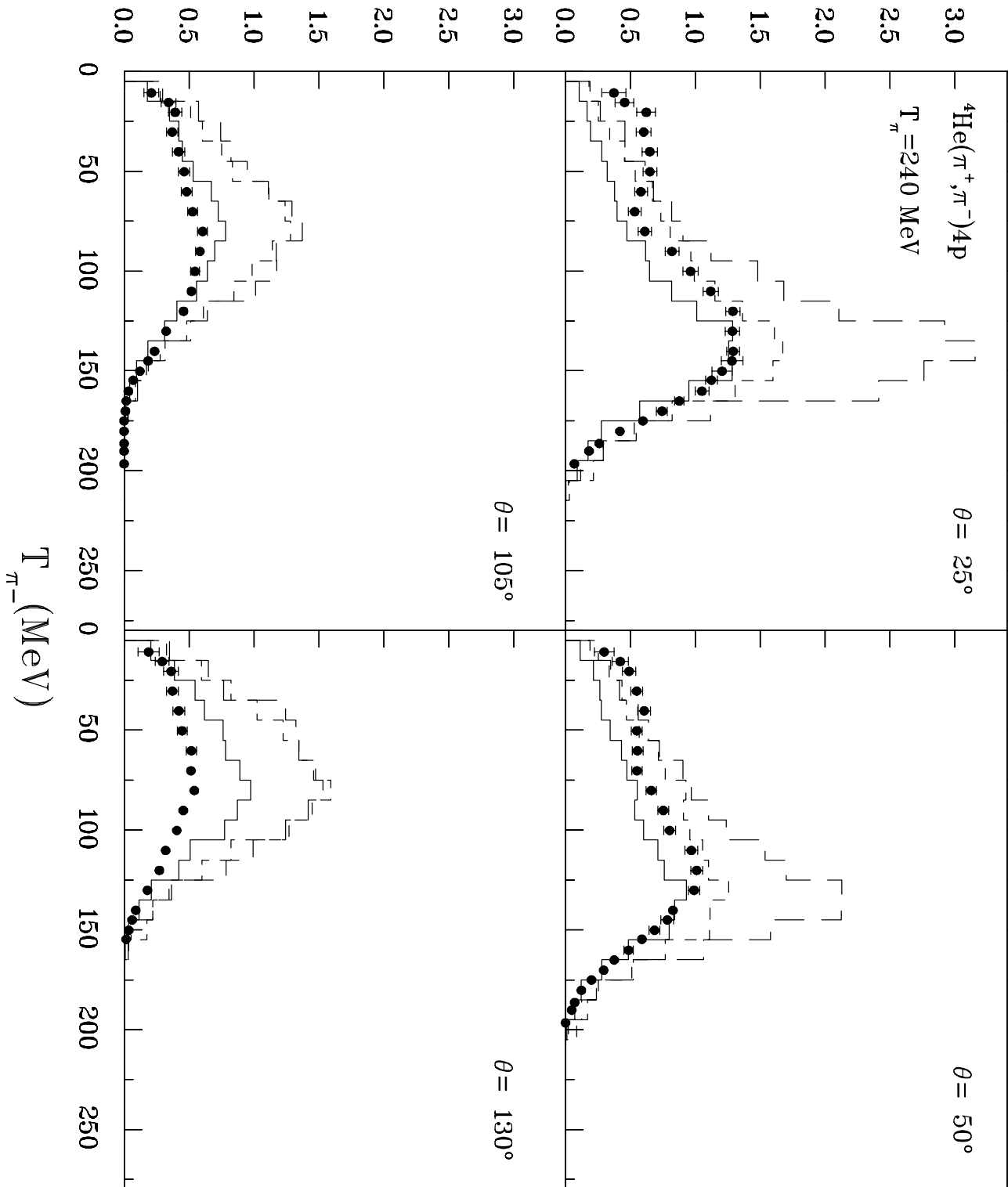


Figure 5: The results of the INC at incident pion energy of 240 MeV. The solid histogram represents the results including FSI and absorption factor, the short dashed histogram has no absorption. The long dashed histogram represents the results of taking two neutrons only.

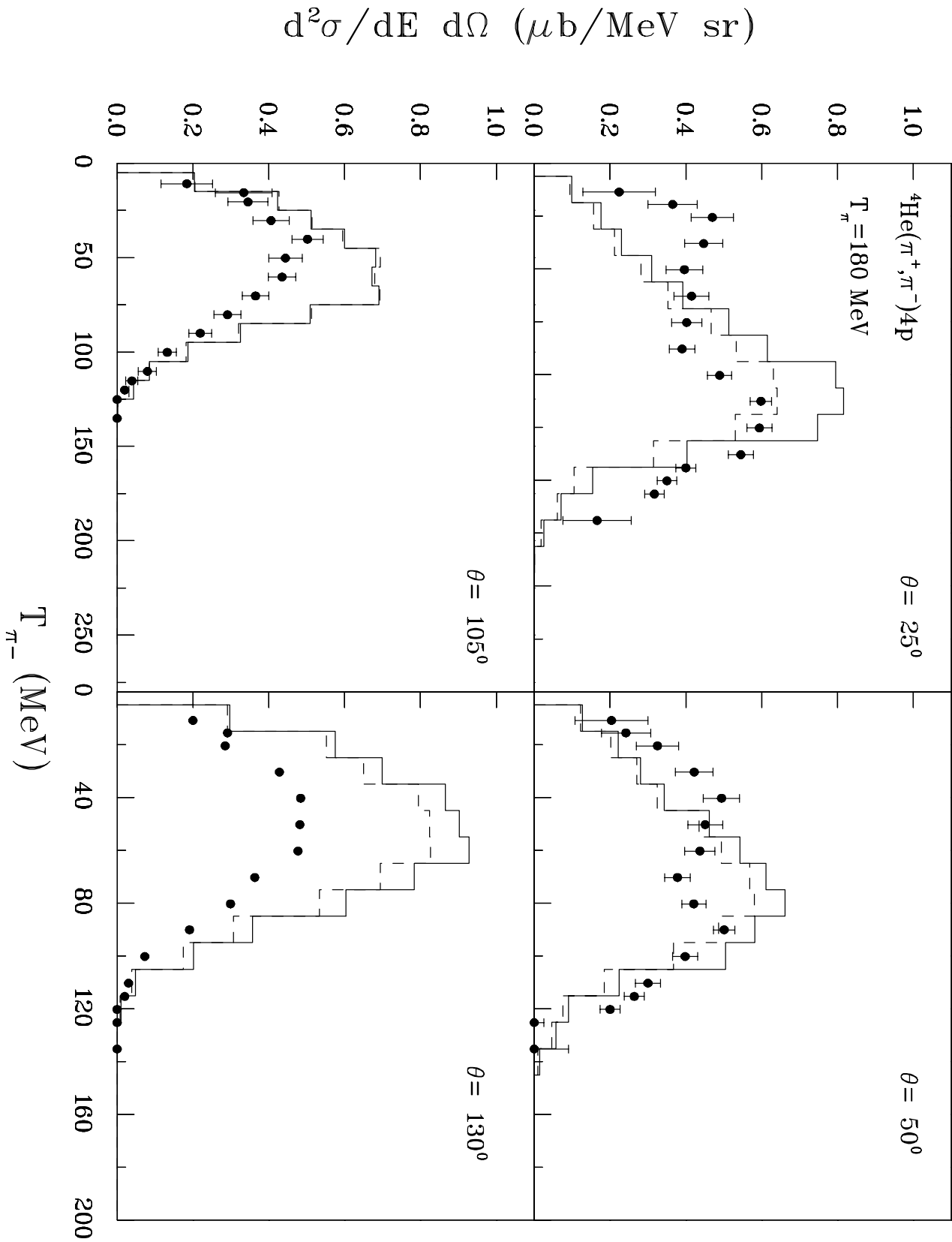


Figure 6: The same as Fig. 4 but at incident pion energy 180 MeV.

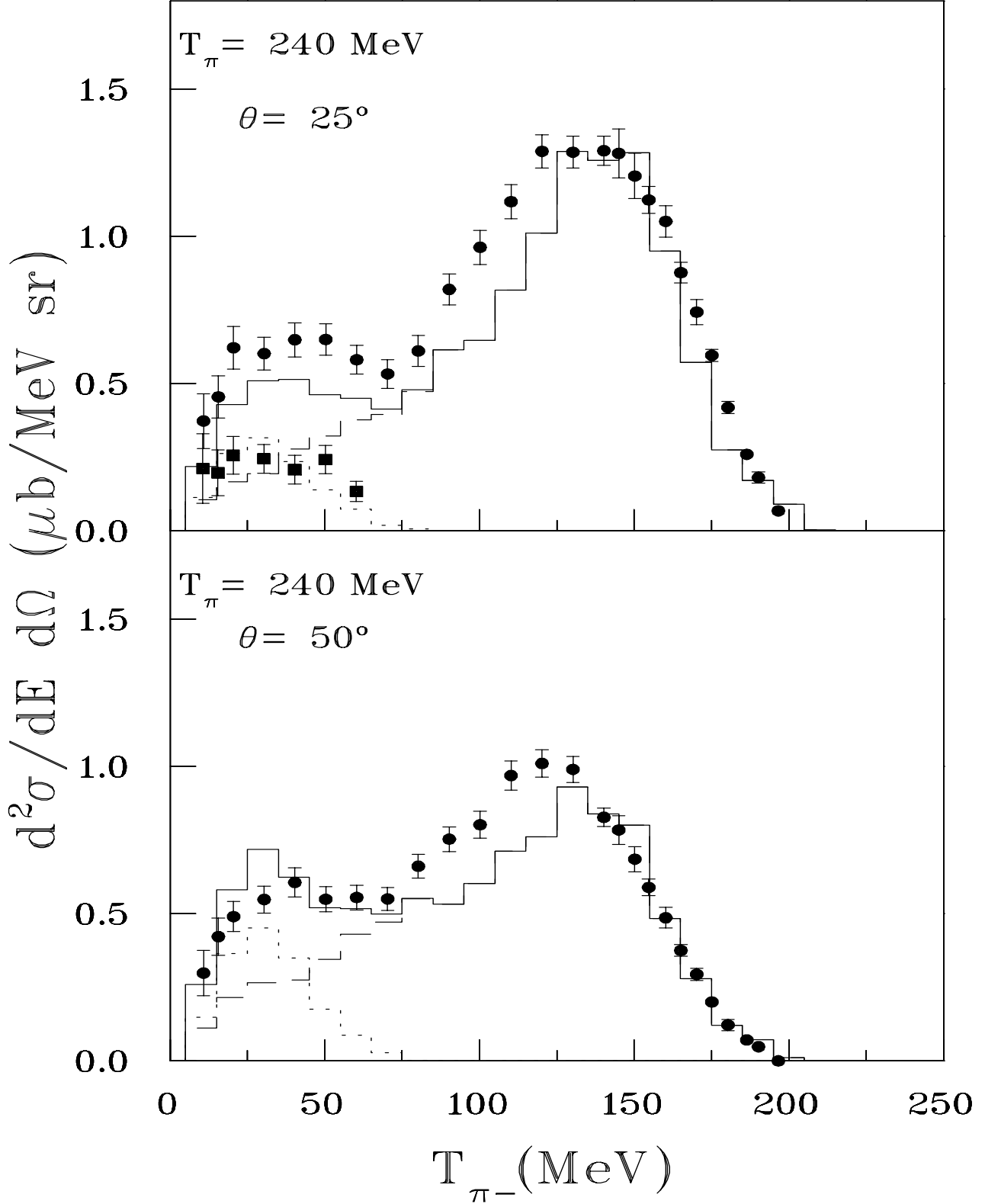


Figure 7: The results of doubly differential cross section at 240 MeV. The solid histogram shows our results with FSI, absorption with pion production, while the dashed line shows the result without pion production. The dotted line shows the pion production cross section alone. The data given in the solid squares are the production cross sections from Ref. [10] multiplied by two.

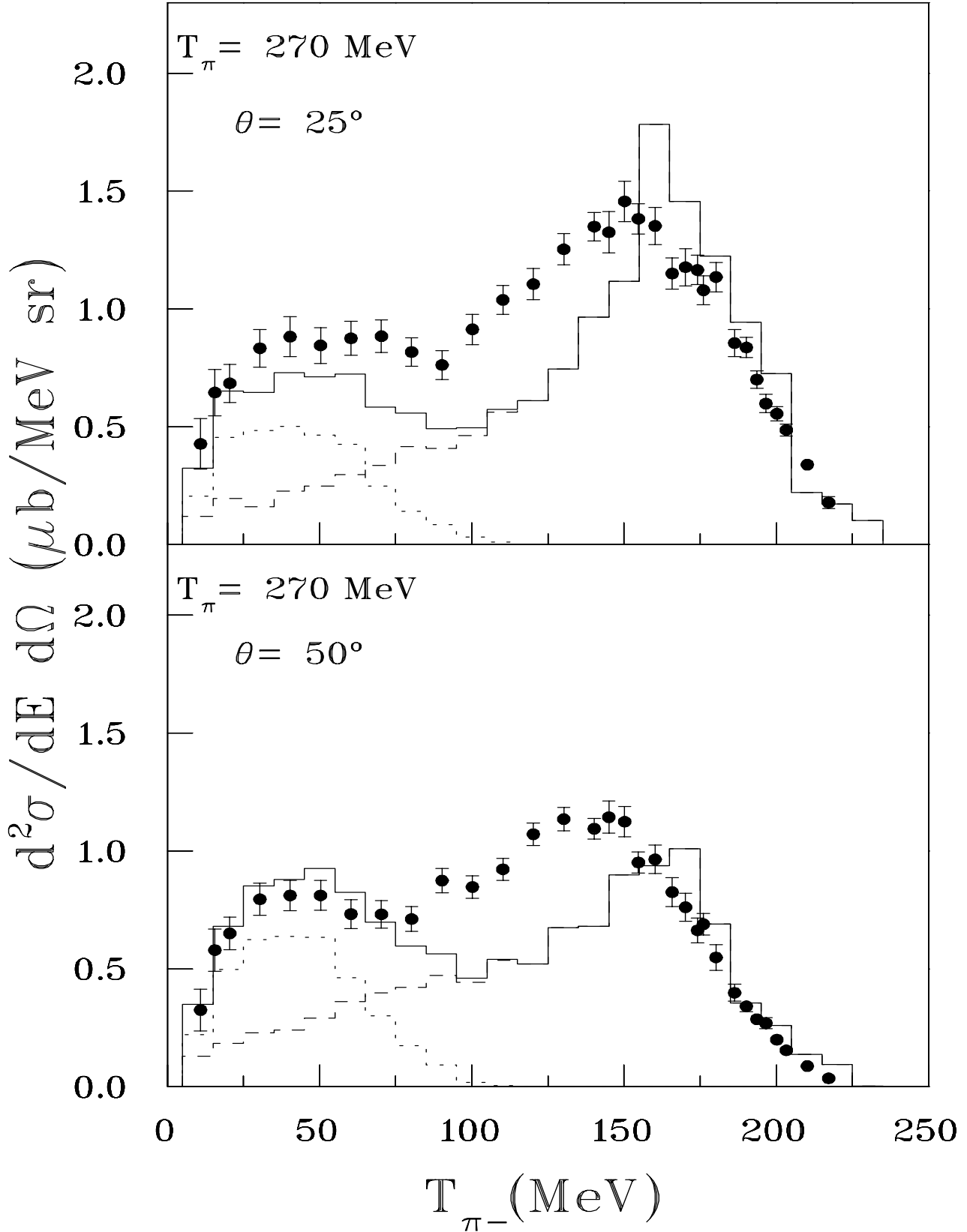


Figure 8: The same as Fig. 8 but at an incident energy of 270 MeV.

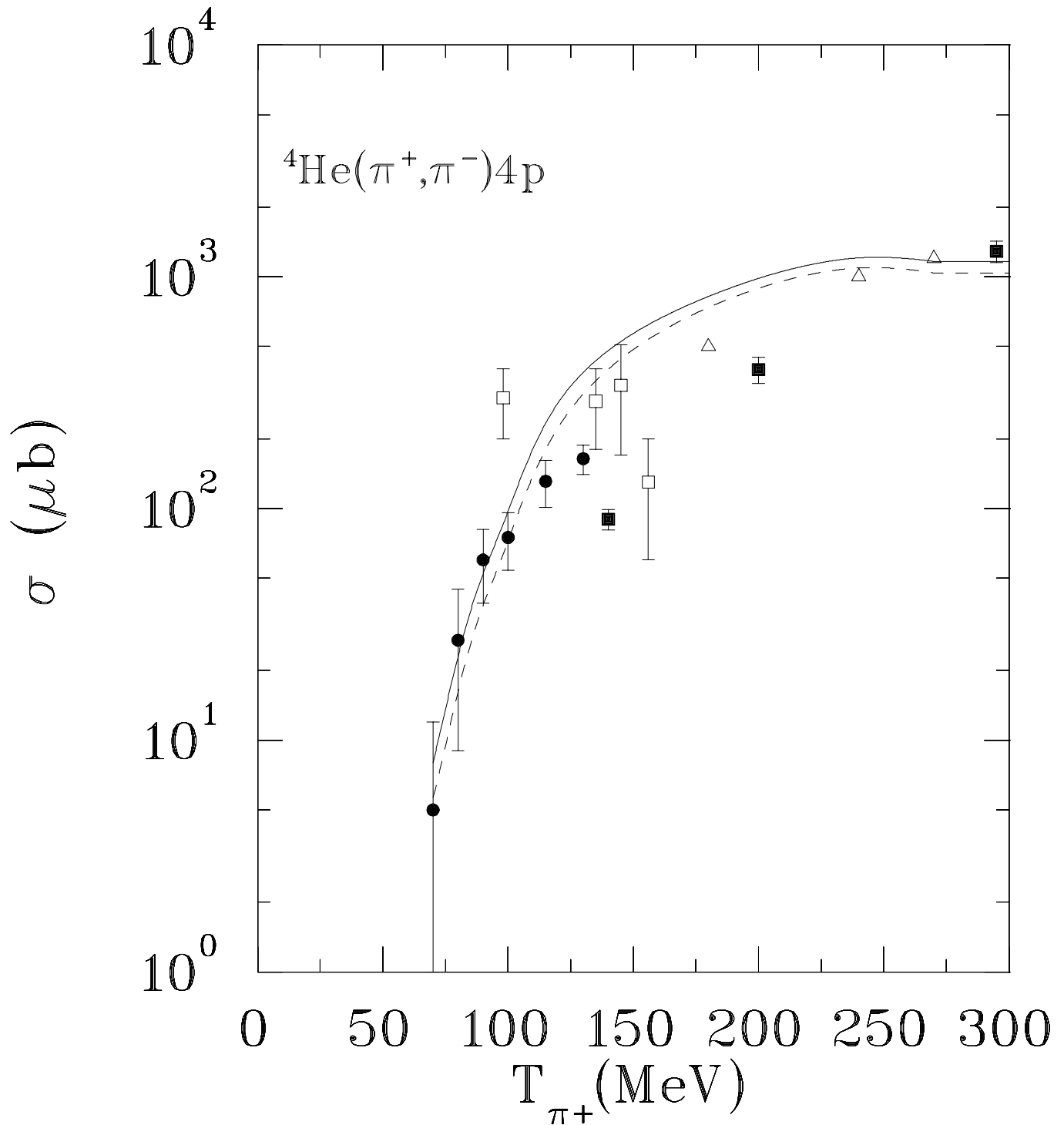


Figure 9: Total DCX cross section for ${}^4\text{He}(\pi^+, \pi^-)4\text{p}$. The solid line shows the results including FSI and absorption factors, while the dashed line is without FSI. The experimental data were taken from [8] (solid circles), [9] (open triangles), [21] (open squares) and [22] (solid squares).